Effects of Fluid Density on a Poly(dimethylsiloxane)-Based Junction in Pure and Methanol-Modified Carbon Dioxide

Chase A. Munson, Phillip M. Page, and Frank V. Bright*

Department of Chemistry, Natural Sciences Complex, University at Buffalo, The State University of New York, Buffalo, New York 14260-3000

Received September 29, 2004; Revised Manuscript Received December 2, 2004

ABSTRACT: We report on the behavior of a three-armed, poly(dimethylsiloxane) (PDMS)-based junction that is site-selectively labeled with a single fluorescent dansyl reporter group (dansyl junction, DJ) in (i) pure CO_2 at 308 K as a function of CO_2 density and (ii) a binary mixture of CO_2 and 3 mol % methanol at 313 K as a function of mixture density. The DJ results are compared to those of dansylpropylsulfonamide (DPSA)—a dansyl reporter molecule without any PDMS segments. In pure CO_2 at low fluid densities, the local microenvironment sensed by the dansyl residue in DJ appears to be rich in PDMS, indicating that the solvent quality is poor and the PDMS segments interact strongly with the dansyl residue. Increasing the CO_2 density increases the solvent quality, and PDMS segments become better solvated by the CO_2. At the highest CO_2 densities studied, the solvent quality begins to decrease again, resulting in a local increase in the PDMS composition around the average dansyl residue. Results from steady-state anisotropy measurements suggest the presence of DJ aggregates in the fluid phase at low CO_2 densities. As the CO_2 density is increased, these aggregates are disrupted, and isolated DJ molecules appear to be the major species in the fluid phase above a reduced CO_2 density of ~1.5 and up to ~1.9. DJ aggregates are present in the CO_2/methanol mixture at all fluid densities studied. At low mixture densities there is enrichment in the local methanol concentration surrounding the dansyl residue in DJ in comparison to isolated DPSA molecules under equivalent mixture densities. Thus, it appears as if the PDMS segments in DJ augment/enhance the methanol concentration surrounding the dansyl reporter group in DJ. Together these results demonstrate the dramatic role fluid density and composition can play in tuning the local microenvironment that surrounds a polymeric junction point.

Introduction

Supercritical fluids exhibit liquidlike densities and gaslike mass transfer, making them attractive solvents for extractions, separations, and reactions.[1−9] In addition, above the system critical temperature (T_c), small pressure changes allow one to continuously tune a supercritical fluid's physicochemical properties (e.g., density, dielectric constant, and refractive index).

Carbon dioxide is the most widely used supercritical fluid because it exhibits easy to access critical conditions (critical pressure $P_c = 73.8$ bar, critical temperature $T_c = 304.3$ K), it is easily recyclable, environmentally benign, inexpensive, nonflammable, and nontoxic, and it can be easily separated from a reaction medium.[1−9] Despite its many attractive characteristics, supercritical CO_2 ($scCO_2$) exhibits a relatively low solvent power in comparison to normal liquids such as methanol or even hexane. As a result, it can be difficult to solubilize polar or high molecular weight species in useful quantities in pure $scCO_2$. For example, Laintz et al. reported that the solubility of alkylmetal chelates in pure $scCO_2$ was 10^{-5} g/g, a quantity much lower than is needed for cost-efficient, large-scale extractions.[10] The solubility of certain chemical species can be improved by the covalent attachment of CO_2-philic functional groups.[11] Examples of CO_2-philic functionalities include fluorinated alkanes and ethers, silicones, and poly(carbonate−ether) copolymers.[11−31]

CO_2-philic species have found widespread use.[21−31] For example, functionalization of chelates with CO_2-philic oligomers has resulted in the creation of CO_2-soluble species that can be used to extract heavy metals such as Hg, As, Pb, and Pt.[21,22] Addition of a CO_2-philic perfluoroether oligomeric tail to the poorly CO_2 soluble coenzyme nicatinamide adenine dinucleotide increased the activity of horse liver alcohol dehydrogenase in $scCO_2$.[23] Fluorinated styrene and acrylic polymers have been used to modify the bulk viscosity of CO_2.[24,25] CO_2-philic polymers and oligomers have also been used in the design of effective CO_2-soluble surfactants and stabilizers.[26−31] To improve the development of hybrid reagents that contain CO_2-philic and CO_2-phobic segments such as those described above requires molecular-level insights into how these segments interact with each other as one adjusts the solvent quality.

Fluorescence spectroscopy is a useful tool for studying the local microenvironment that surrounds a fluorescent probe molecule (i.e., the cybotactic region), exploring polymer dynamics on nanosecond and subnanosecond time scales, and studying dilute polymer solutions, polymer melts and blends, and entangled or cross-linked polymer networks.[32−45] Previously, we reported on the dynamics of a poly(dimethylsiloxane) (PDMS)-based, three-armed junction that contained a single, focally located fluorescent dansyl reporter group (the dansyl junction, DJ) in a series of normal liquids as a function of solvent quality (good, Θ, and poor) and temperature.[46] In the current work, we report on the behavior of DJ and dansylpropylsulfonamide (DPSA) (Figure 1) when they are dissolved in (i) pure CO_2 at a reduced temperature ($T_r = T_{exp}/T_c$) of 1.02 between a reduced density ($\rho_r = \rho_{exp}/\rho_c$) of 0.34 and 1.90 and (ii) a binary mixture of CO_2 with 3 mol % methanol at $T_r = 1.04$ between $\rho_r = 0.40$ and $\rho_r = 1.40$. These two systems were chosen

* To whom correspondence should be addressed. Phone: (716) 645-6800 ext 2162. Fax: (716) 645-6963. E-mail: chefvb@acsu.buffalo.edu.

10.1021/ma047989k CCC: $30.25
Published on Web 01/29/2005

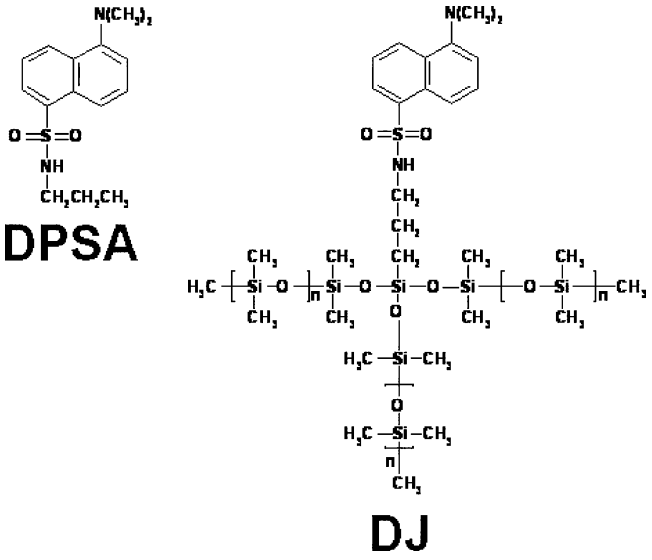

Figure 1. Chemical structures of DPSA and the three-arm PDMS-based junction bearing a single pendant dansyl residue (DJ).

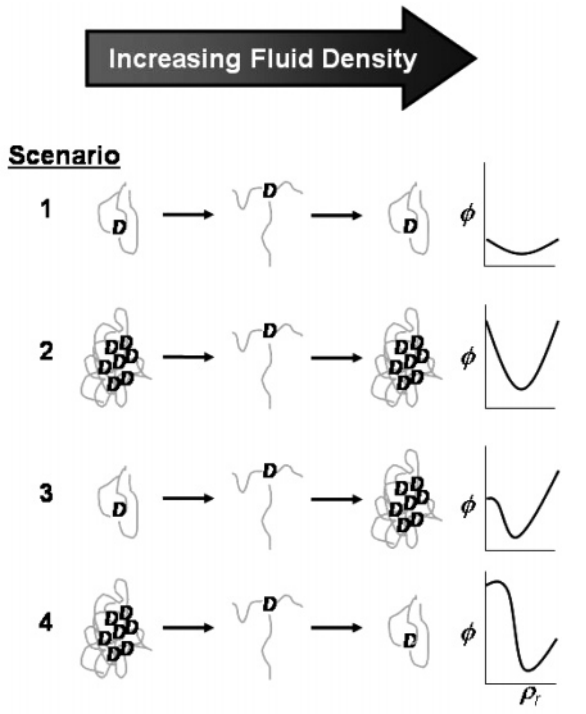

Figure 2. Four potential scenarios for the density-dependent behavior of DJ. The direction of increasing fluid density is indicated by the large arrow. A qualitative prediction of the rotational correlation time, ϕ, vs reduced fluid density for each scenario is given on the right-hand side of the figure.

because PDMS is soluble in pure $scCO_2$,[47,48] CO_2 density has been shown to significantly affect the tail−tail dynamics and aggregation properties of linear PDMS polymers,[43,49,50] and methanol is a poor solvent for PDMS.[51] The goal of this work is to determine how fluid density and composition affect a branched, polymer-based junction molecule.

Theory Section

Consider a molecule such as DJ (Figure 1) dissolved in a tunable fluid. Figure 2 illustrates four possible scenarios as the fluid density is adjusted; there are many other scenarios (vide infra). In scenario 1, isolated DJ molecules are the major species in the fluid phase, and intermolecular DJ−DJ interactions are weak at all fluid densities. At low fluid densities, the PDMS chain segments collapse around the dansyl (D) reporter. As the fluid density is increased, the solvent quality increases, and the PDMS segments become better solvated by the fluid, exposing the dansyl residue to the fluid. Further increases in the fluid density result in the PDMS segments again collapsing around the dansyl residue. In scenario 2, the DJ molecules at low fluid density interact strongly and exist as aggregates. Increasing the fluid density disperses these aggregates, and individual DJ molecules become well solvated in the intermediate density region. At higher fluid densities, PDMS−PDMS interactions are favored, and the DJ molecules again aggregate. Scenario 3 begins with isolated DJ molecules at the lowest fluid densities. Like the other scenarios, an increase in the fluid density causes the fluid's solvent quality to increase, and DJ molecules become well solvated, here in their isolated form. High fluid densities again result in the formation of DJ aggregates. The final scenario, scenario 4, begins with DJ molecules in an aggregated form at low fluid densities. The DJ aggregates are dispersed as the fluid density is increased, and individual DJ molecules become well solvated with increasing fluid density. As the fluid density is increased the PDMS segments collapse around the dansyl residues.

How can we distinguish between these possible scenarios?

In dilute solution one can study aggregation by recording the steady-state fluorescence anisotropy, r:[52,53]

$$r = (I_{||} - I_{\perp})/(I_{||} + 2GI_{\perp}) \quad (1)$$

In this expression $I_{||}$ and $I_{\perp}$ represent the parallel and perpendicular components of the polarized fluorescence intensity when the sample is excited with vertical polarized electromagnetic radiation.[52,53] G is an instrumental factor that corrects for differing sensitivities of the sample cell windows, lenses, optical filters, gratings, and detector envelope to the emission polarization. In the simplest case of isotropic rotational reorientation,[54] r is given by the Perrin equation:[52]

$$r = r_0/[1 + (\tau/\phi)] \quad (2)$$

where r_0 is the fluorophore limiting anisotropy, τ is the excited-state fluorophore lifetime, and ϕ is the fluorophore rotational reorientation time. r_0 is measured for the fluorophore in the absence of rotational diffusion, and is determined experimentally in vitrified solution (e.g., glycerol at 223 K). Under our experimental conditions, the dansyl residue r_0 value is 0.325.[55]

The Debye−Stokes−Einstein expression[52a,b]

$$\phi = \eta V/RT \quad (3)$$

provides a link between ϕ and the volume, V, of the rotating fluorophore along with anything attached *to* the fluorophore (e.g., a junction).[54] R and T are the gas constant and Kelvin temperature, respectively. A variation of eq 3 is often used to estimate the rotational reorientation time for "globular" species:[52,53]

$$\phi = \eta M/RT(v_s + s) \quad (4)$$

In this expression, M is the molecular weight of the

rotating body/entity, v_s is its specific volume, and s is the solvation (g of solvent/g of solute).

The right-hand side of Figure 2 illustrates the qualitative effects of reduced fluid density (ρ_r) (related to solvent viscosity) on ϕ for each scenario. In the current work we use density-dependent steady-state emission and fluorescence anisotropy experiments to estimate the behavior of DJ in pure and cosolvent-modified CO_2.

Experimental Section

Chemicals and Reagents. HPLC grade toluene, dansyl chloride, and propylamine were obtained from Aldrich and used as received. Ethanol (dehydrated, 200 proof) was purchased from Pharmco. A binary mixture of supercritical fluid chromatography grade CO_2 and 3 mol % methanol was obtained from Scott Specialty Gases.

Three-Arm Junction Synthesis. A three-arm PDMS-based polymer junction bearing a single dansyl fluorophore (DJ in Figure 1) was custom synthesized, purified, and characterized by Polymer Source Inc. The synthesis involved the anionic polymerization of hexamethylcyclotrisiloxane followed by termination with purified *N*-(triethoxysilylpropyl)-dansylsulfonamide (D-TriEOS). The desired product was separated from undesired species (one- and two-arm polymer and unreacted D-TriEOS) by using a toluene/methanol fractionation step. Triple-detection size exclusion chromatograph (3D-SEC; light scattering, differential refractive index, and intrinsic viscometry detection) was used to characterize the junction. DJ exhibited the following characteristics: absolute molar mass $M_n = 15000$ g/mol and $M_w/M_n = 1.20$.

DPSA Synthesis. Dansyl chloride was reacted under ambient conditions in the dark with a 25-fold molar excess of pure propylamine for a period of 7−10 days. Propylamine was removed by evaporation with a stream of N_2, leaving behind crude DPSA. The DPSA was purified by column chromatography.

Fluorescence Instrumentation. An SLM-AMINCO model 48000 MHF (Spectronic Instruments) was used to record the fluorescence spectra and steady-state fluorescence anisotropies. The standard 90° excitation-detection geometry was used. A He−Cd laser (Omnichrome, 325 nm) served as the excitation source. A 330 ± 15 nm interference filter (Omega Optical) was placed in the laser beam path to minimize laser superradiance from reaching the detection system. Emission wavelength selection was performed by using a single-grating monochromator with a 4 nm spectral band-pass. Steady-state fluorescence anisotropy experiments were performed by using a 425 nm long pass filter (Oriel). All emission spectra and anisotropy data were background corrected by using the PeakFit software package (Jandel Scientific) during spectral analysis or by using appropriate blanks.

The time-resolved fluorescence intensity decay profiles were recorded by using an IBH model 5000W SAFE time-correlated single-photon-counting fluorescence lifetime instrument. A N_2-filled flash lamp (337 nm, 40 kHz repetition rate) was the excitation source. Single-grating monochromators were used to select the desired wavelengths. For these experiments, all intensity decay measurements were collected at 470 nm (spectral band-pass = 32 nm) under magic angle polarization conditions to eliminate any bias arising from fluorophore rotational reorientation.[56] The typical time resolution for an experiment was 0.096 ns/channel, and 1024 multichannel analyzer (MCA) channels were used to record the decay trace. To avoid pulse pileup, the count rate at all detectors was always maintained below 2% of the flash lamp repetition rate. Data were acquired until there were at least 10^4 counts in the peak MCA channel. The time-resolved intensity decay data were analyzed using Globals WE (Globals Unlimited), a commercially available global analysis software package.

High-Pressure Spectroscopy. The high-pressure spectroscopy system[57] consists of a microprocessor-controlled syringe pump (Isco model 260-D) that is charged with the fluid of interest (e.g., pure CO_2 or methanol-modified CO_2), stainless steel tubing and valves, and a stainless steel high-pressure optical cell with four fused silica optical windows. The system pressure is regulated by the Isco pump (±2 psia), and it is determined with a calibrated analogue Heise gauge. Temperature control within the high-pressure optical cell (±0.1 K) is achieved by using four 100 W cartridge heaters (Omega Engineering, model CIR-1031) and a thermocouple probe (Omega Engineering, model RID-860) located within the cell body, and a microprocessor-based temperature controller (Omega Engineering, model CN 76000 series).

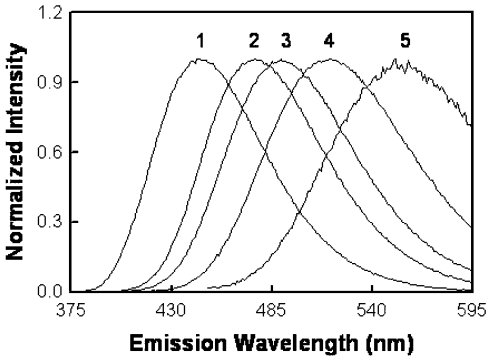

Figure 3. Normalized steady-state emission spectra for DPSA dissolved in (1) *n*-hexane, (2) toluene, (3) ethyl acetate, (4) methanol, and (5) water.

Sample Preparation for Fluorescence Studies. Samples were prepared by micropipetting a small aliquot (<100 μL) of DJ or DPSA dissolved in toluene into a clean high-pressure optical cell. Residual solvent was removed by gently flushing the cell with Ar gas. Prior to initial pressurization, the cells were brought to temperature and flushed with pure CO_2(g) or Ar(g) for a period of 10 min to remove residual O_2 and toluene. All samples were prepared so that the final fluorophore concentration was ≤20 μM.

Fluid Properties. The pure CO_2 density at a given P and T was determined by using a modified Benedict−Webb−Rubin equation of state.[58] The pure CO_2 viscosities at a given T and P were taken from Fenhour et al.[59] The density and viscosity of the binary methanol/CO_2 mixtures at a given T and P were determined by using the Peng−Robinson equation of state and the Ely and Hanley technique with a density-dependent noncorrespondence factor as described by Foster and coworkers.[59,60]

Statistics. All results are the average of at least three separate experiments. Results are reported as the average for a series of experiments under a given set of conditions. All error bars represent ±2 standard deviations (95% confidence level).

Results and Discussion

Steady-State Fluorescence from DPSA in Normal Liquids. The steady-state emission spectra from dansyl residues are solvent dependent.[61] In nonpolar solvents the emission maximum appears in the blue spectral region; the spectra systematically shift to the green as the solvent becomes more polar. The dansyl residue's absorbance maxima are largely independent of solvent in comparison to the emission maxima.[61] This solvatochromic behavior is often used to assess the local microenvironment surrounding dansyl reporter molecules. For example, dansyl residue emission has been used previously as a probe to study silica surfaces,[61b,c,h] glass fibers,[61k,m] polymeric films,[61f,g] and sol−gel-derived xerogels.[61l]

Figure 3 presents a series of normalized steady-state emission spectra for DPSA dissolved in five liquid solvents at 298 K. One can see that the DPSA spectra shift from the blue toward the red as the solvent polarity increases. We use this solvatochromic behavior as a tool

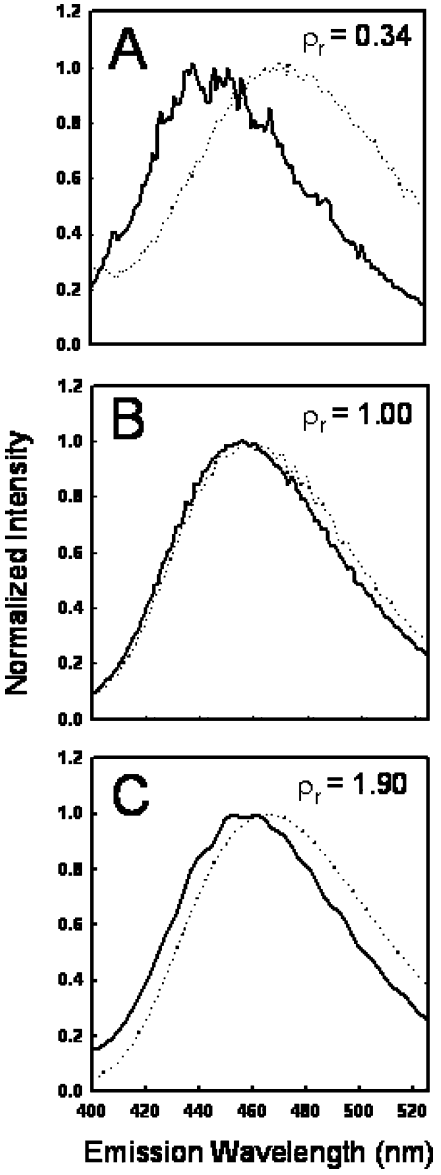

Figure 4. Normalized steady-state emission spectra for 20 μM DPSA (—) and DJ (···) in pure supercritical CO_2 at T_r = 1.02: (A) ρ_r = 0.34, (B) ρ_r = 1.00, (C) ρ_r = 1.90.

to estimate the cybotactic region that surrounds DPSA and the dansyl residue within DJ.

Steady-State Fluorescence from DPSA and DJ in Pure $scCO_2$. Figure 4 presents typical emission spectra for dilute solutions of DPSA (—) and DJ (···) in pure $scCO_2$ (T_r = 1.02) at ρ_r = 0.34, 1.00, and 1.90. The emission spectra depend on the dansyl residue's attachment site (propyl vs PDMS-based junction) *and* the CO_2 density. Figure 5 presents the density-dependent emission maxima for DPSA and DJ in pure $scCO_2$. The curves that pass through the data are an aid to the eye; they do not represent a particular model. The two horizontal lines are benchmarks, denoting the DPSA emission maxima in pure liquid *n*-hexane (-·-) and pure methyl-terminated PDMS (M_n = 2000 g/mol) (-···-) at 308 K. The emissive behavior of DJ and DPSA in $scCO_2$ can be best described by dividing the full density range into three subregions: $\rho_r \leq 0.7$, $0.7 < \rho_r < 1.2$, and $\rho_r \geq 1.2$.

At a reduced density below ~0.7, the DPSA emission maximum is blue shifted in comparison to that of the dansyl residue in DJ at an equivalent CO_2 density. This is most evident in Figure 4A at ρ_r = 0.34, where the

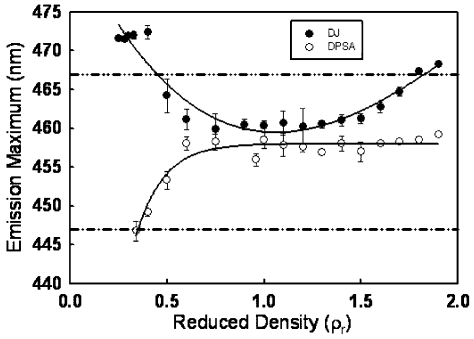

Figure 5. Summary of the CO_2 density-dependent emission maxima for DPSA (○) and DJ (●) at T_r = 1.02. DPSA emission maxima in pure liquid *n*-hexane (-·-) and pure methyl-terminated PDMS (M_n = 2000 g/mol) (-···-) at 308 K are provided as a benchmark.

difference in emission maxima is ~30 nm. At this CO_2 density, DPSA is reporting from a cybotactic region akin to liquid *n*-hexane while the dansyl residue in DJ reports/senses a cybotactic region that is more like PDMS. These results are consistent with the dansyl residue in DJ sensing a PDMS-rich microenvironment in this low-density regime. Upon increasing the CO_2 density from ρ_r = 0.34 to $\rho_r \approx 0.7$, we see a progressive increase in the polarity sensed by the DPSA molecules, and a concomitant decrease in the polarity sensed by the dansyl residues in DJ. These results indicate that the environment surrounding the dansyl residue in DJ becomes less PDMS-like and more CO_2-like as the CO_2 density is increased between ρ_r = 0.34 and $\rho_r \approx 0.7$. Between a reduced density of ~0.7 and ~1.2, the DPSA and DJ emission spectra are very similar to one another (cf. Figure 4B), and increasing the CO_2 density over this range has little effect on the polarity sensed by DPSA or the dansyl residue in DJ. As we increase the CO_2 reduced density beyond ~1.2, we continue to see little change in the microenvironment sensed by the DPSA molecules; however, we note a systematic shift in the dansyl residue emission in DJ toward an environment that is progressively more PDMS-like in comparison to the environment sensed by DPSA in $scCO_2$. Figure 4C illustrates this shift for DPSA and DJ at ρ_r = 1.9.

The DPSA emission spectra track the effects of CO_2 density on the dansyl residue alone. The DJ emission spectra track the effects of CO_2 density on the local microenvironment sensed by the dansyl residue within DJ. Consequently, the density-dependent *differences* in fluorescence emission between the dansyl residue emission in DJ and DPSA can be assigned to the effects of CO_2 density on the PDMS chains that make up the PDMS-based junction. Figure 6 presents the differences in DJ and DPSA emission maximum ($DJ_{max} - DPSA_{max}$) as a function of CO_2 reduced density (○).

In a related experiment, Melnichenko et al. used small angle neutron scattering to study the pressure- and temperature-dependent phase behavior of PDMS dissolved in $scCO_2$.[62] In their studies with a linear PDMS polymer (M_n = 47000 g/mol) at 305 K (near the upper critical solution temperature, 304 K) in $scCO_2$, the authors observed density-induced changes in PDMS radius of gyration and correlation lengths. Pertinent correlation length (ξ) data from Melenchenko et al. have been rescaled in terms of reduced CO_2 densities in Figure 6 (●). At the lowest CO_2 densities studied by Melenchenko et al., $\rho_r \simeq 2.0$, ξ is high. As the CO_2 density is increased from $\rho_r \simeq 2.0$ to $\rho_r \approx 2.2$, ξ drops,

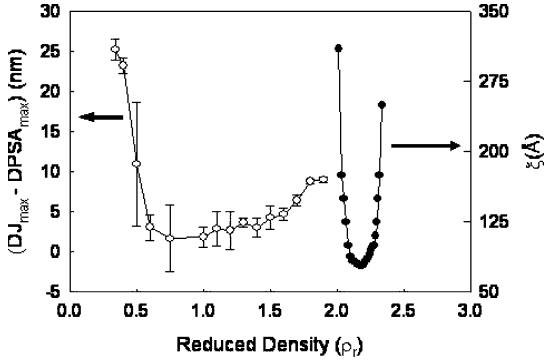

Figure 6. Difference in the CO_2 density-dependent emission maximum between DJ and DPSA ($DJ_{max} - DPSA_{max}$) at $T_r = 1.02$ (○). Density-dependent correlation length (ξ) for linear PDMS ($M_n = 47000$ g/mol) at $T_r = 1.00$ (●). Reprinted from ref 62. Copyright 1999 American Chemical Society.

reaching a minimum at $\rho_r \simeq 2.2$. As the CO_2 density is increased from $\rho_r \simeq 2.2$ to $\rho_r \approx 2.4$, the correlation length again increases. Melenchenko et al. explained these results in terms of the approach to an upper critical solution pressure (density) (UCSP(D)) in the lower density region where the system exhibits pressure (density)-induced phase demixing, Θ conditions at $\rho_r \simeq 2.2$, and approach to a lower critical solution pressure (density) (LCSP(D)) at the higher CO_2 densities where the system again exhibits pressure (density)-induced phase demixing.

Despite the inherent differences between our junction and the system studied by Melenchenko et al. (linear vs branched, molecular weight, measurement techniques), the similarity in the shape of our differential dansyl emission maximum vs ρ_r and the ξ vs ρ_r data causes us to suggest that adjacent "PDMS arms" surrounding the dansyl residue in DJ are undergoing similar transitions in comparison to linear PDMS molecules in $scCO_2$. Specifically, at low CO_2 densities the PDMS−PDMS interactions dominate, and the PDMS arms collapse within the junction to surround the dansyl residue. Under these conditions the dansyl probe molecule(s) sense and report from a "PDMS-like" environment. As the CO_2 density increases, the system passes through a UCSD, CO_2 becomes a "good"/better solvent for PDMS, DJ is well solvated, and the dansyl reporter molecules sense and report from an environment that is "CO_2-like". Further increases in CO_2 density cause the system to approach or pass an LCSD, and the solvent quality of CO_2 for PDMS again decreases. Under these conditions, the dansyl residue in DJ once again reports from a "PDMS-rich" microenvironment.

Evidence for DJ Aggregation in Pure $scCO_2$. The steady-state emission results (vide supra) are consistent with several scenarios. Figure 2 illustrates four possible scenarios that are consistent with the data presented in Figures 3−6. Other scenarios can certainly be considered. On the right-hand side of Figure 2 we present simple *qualitative* predictions of how ϕ would change as a function of CO_2 density (i.e., increasing fluid viscosity) for each scenario. Aggregation of the DJ molecules would result in the highest ϕ values, followed by lower values for nonaggregated DJ molecules with collapsed PDMS arms. The lowest ϕ values are anticipated for well-solvated, isolated DJ molecules where there is minimal interaction between the PDMS arms and a focally located dansyl reporter molecule.

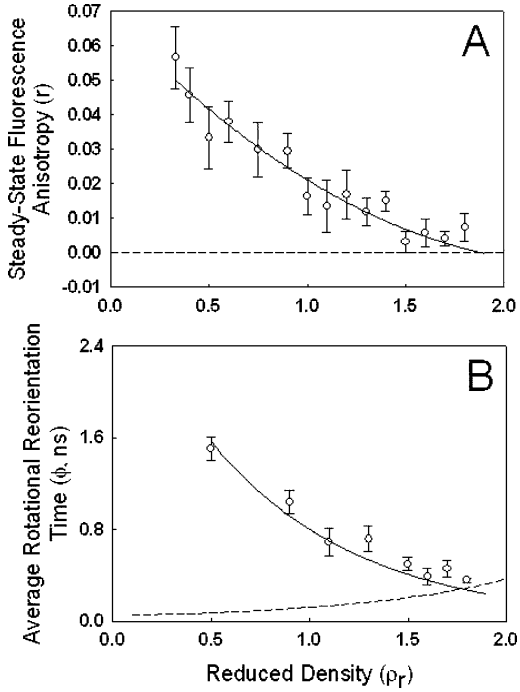

Figure 7. Density-dependent rotational reorientation dynamics for DJ in pure CO_2 at $T_r = 1.02$: (A) density-dependent steady-state fluorescence anisotropy (r), (B) density-dependent average rotational reorientation time (ϕ). The dashed line represents an estimate of N using eq 4 for isolated DJ molecules with an absolute molecular weight of 15000, $\nu_s = 1.03$ mL/g, and $s = 0$.

Figure 7A presents the density-dependent r for DJ in pure $scCO_2$. These data have been carefully corrected for any background and polarization anomalies by using a second high-pressure optical cell that contained an analogue of DJ without any dansyl residue under identical conditions. The solid line that passes through the data is provided only to guide the reader's eye; it is not a model. At low CO_2 densities/viscosities the observed fluorescence anisotropy is relatively high. As the CO_2 density increases, the anisotropy decreases significantly.

The DJ excited-state lifetime was determined by recording the time-resolved intensity decay traces and fitting these data to a unimodal continuous lifetime distribution model.[63] The mean excited-state lifetimes ranged from 12.5 ± 0.2 ns at $\rho_r = 0.5$ to 20.9 ± 0.2 ns at $\rho_r = 1.9$ (results not shown).

We calculated the average DJ ϕ from these r and τ data using eq 2. Figure 7B presents the average density-dependent ϕ (points) for DJ in $scCO_2$. The solid line is a guide to the reader's eye; it is not a model. To *estimate* the density-dependent behavior of isolated DJ molecules in $scCO_2$, we used eq 4 and assumed a globular molecule with a molecular weight equal to the DJ absolute molar mass ($M = 15000$ g/mol) and density-independent values for ν_s and s (i.e., $\nu_s = 1.03$ mL/g,[64] and $s = 0$). The dashed curve in Figure 7B is the result of this estimate. Although the intrinsic limitations of the steady-state anisotropy experiments[54] and our assumptions preclude quantitative conclusions, differences between the experimental and estimated ϕ can be used to qualitatively sense density-dependent changes in DJ.

For example, if DJ were behaving as an isolated molecule in $scCO_2$, ϕ should increase with increasing ρ_r (increasing η). The experimental results for DJ are not consistent with this scenario. Specifically, the DJ ϕ is

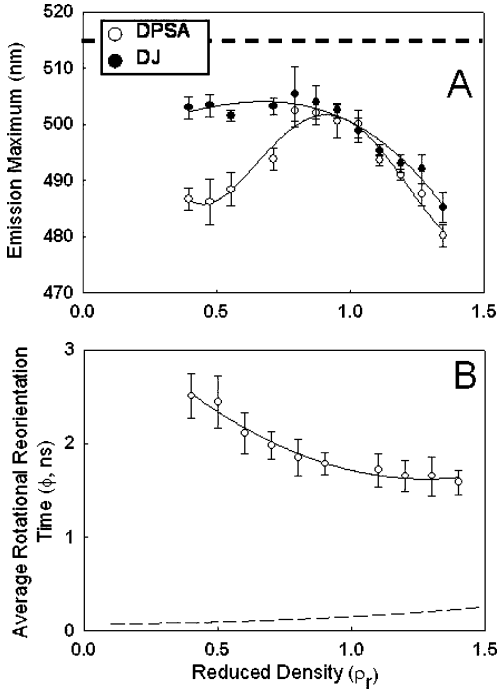

Figure 8. Density-dependent fluorescence from DJ in a binary mixture of 3 mol % methanol and CO_2 at $T_r = 1.04$: (A) density-dependent emission maxima for DPSA (○) and DJ (●), (B) density-dependent average rotational reorientation time (ϕ). The dashed line in panel B represents an estimate of ϕ using eq 4 for isolated DJ molecules with an absolute molecular weight of 15000, $\nu_s = 1.03$ mL/g, and $s = 0$.

substantially higher than the predicted ϕ for isolated DJ molecules at low CO_2 densities, and the experimental ϕ approaches the estimated ϕ at higher CO_2 densities. This difference between the experimental and predicted ϕ at low CO_2 densities is consistent with DJ aggregates at low CO_2 densities. Similar aggregation behavior was seen previously for 6-(1-pyrenyl)hexyl-11-(1-pyrenyl)undecanoate dissolved in pure supercritical CO_2 at low fluid densities.[65] As the CO_2 density is increased, these DJ aggregates appear to dissociate. It appears as if there are isolated DJ molecules above $\rho_r \approx 1.5$.

DPSA and DJ in Methanol-Modified CO_2. Figure 8 summarizes the density-dependent behavior of DJ in a binary mixture of CO_2 with 3 mol % methanol at $T_r = 1.04$ between $\rho_r = 0.40$ and $\rho_r = 1.40$. Figure 8A presents the density-dependent emission maxima for DPSA and DJ in CO_2/methanol. The curves that pass through the data are an aid to the eye; they do not represent a particular model. The dashed horizontal line is a benchmark, denoting the DPSA emission maxima in pure liquid methanol at 313 K. The emissive behavior of DJ and DPSA in CO_2/methanol can be best described by dividing the full density range into two subregions: $\rho_r \leq 1.0$ and $\rho_r \geq 1.0$. At the low mixture densities, the DJ emission maximum is red shifted significantly in comparison to that of the dansyl residue in DPSA at an equivalent mixture density. As we increase the mixture reduced density from 0.4 to ~1.0, the difference between the DPSA and DJ emission maxima systematically lessens. These results are consistent with an increase in the *local* methanol composition surrounding the dansyl residues within DJ in comparison to DPSA at equivalent mixture densities. That is, the PDMS segments on the DJ seem to lead to an augmentation of the local composition of methanol surrounding the dansyl residue in DJ at low mixture densities. This effect is greatest at the lowest mixture densities studied. As we increase the mixture reduced density above 1.0, we see that there is no detectable difference between the dansyl residue emissions in DPSA and DJ. This suggests that the local microenvironments surrounding the dansyl residues are similar for DPSA and DJ above a mixture reduced density of ~1.0.

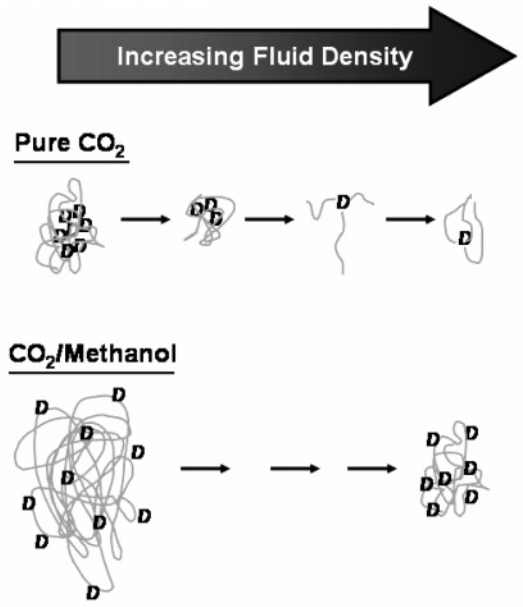

Figure 9. Model describing the effects of fluid density and fluid composition on the behavior of DJ in pure CO_2 and a binary mixture of CO_2 and methanol.

Figure 8B summarizes the effects of mixture density on the average experimental ϕ for DJ in CO_2/methanol (points). An estimate of the density-dependent behavior of isolated DJ molecules in CO_2/methanol is given by the dashed curve. This estimate is based on the same assumptions discussed above for DJ in pure $scCO_2$.[54] The results presented in Figure 8B should be compared to the results presented in Figure 7B for DJ in pure $scCO_2$. At low mixture densities the experimental ϕ is significantly larger than the estimated ϕ for isolated DJ molecules. This result is again consistent with the formation of DJ aggregates at low mixture densities. As the mixture density is increased, there is a decrease in ϕ, which is consistent with some aggregate dissociation or a decrease in aggregate size. However, unlike the behavior seen in pure $scCO_2$, the ϕ in the CO_2/methanol mixture does not reach the estimated value for isolated DJ molecules at the highest mixture densities.

Conclusions

We report on the fluorescence from a poly(dimethylsiloxane)-based, three-armed junction that contains a single dansyl reporter group (DJ) in (i) pure supercritical CO_2 at $T_r = 1.02$ between $\rho_r = 0.34$ and $\rho_r = 1.90$ and (ii) a binary supercritical mixture composed of CO_2 with 3 mol % methanol at $T_r = 1.04$ between $\rho_r = 0.4$ and $\rho_r = 1.40$. The DJ results are compared to those of DPSA, a "junctionless" analogue. Figure 9 summarizes the overall behavior of DJ in the two systems.

In pure CO_2 at low fluid densities and micromolar DJ concentrations, PDMS−PDMS interactions are greater than the PDMS−CO_2 interactions and the DJ molecules aggregate. These aggregates are such that the average dansyl residues see or bury themselves into a PDMS-

rich microenvironment. As the CO_2 density is increased, the fluid quality improves, the DJ aggregates are disrupted, and isolated DJ molecules appear to be the major species in the fluid phase. As the CO_2 density is further increased, isolated DJ molecules continue to be the major species in the fluid phase, but the PDMS segments on these isolated DJ molecules begin to collapse around the dansyl report group as the CO_2 density is increased.

In methanol-modified CO_2 at low mixture densities, PDMS−PDMS interactions are greater than the PDMS−CO_2 or PDMS−methanol interactions and the DJ molecules aggregate. These aggregates are such that the dansyl residues encounter an enhancement in their local methanol concentration in comparison to the DPSA molecules under equivalent mixture densities. Thus, it appears as if the PDMS segments can augment/enhance the methanol concentration surrounding the dansyl reporter group in DJ. One possible explanation for this observation is that the presence of methanol in the fluid phase forces the PDMS segments to aggregate *and* simultaneously exclude the polar dansyl residue from the PDMS-rich core. This is to be compared to the behavior of DJ in pure methanol where we saw the dansyl residues sequestered within the PDMS arms of DJ.[46] As we increase the mixture density, the size of the DJ aggregates appears to decrease, but DJ aggregates are present at all mixture densities.

These results impact the use of catalysts or chelators that are attached to CO_2-philic tethers in pure and cosolvent-modified CO_2.

Acknowledgment. This work was generously supported by the U.S. Department of Energy.

References and Notes

(1) Johnston, K. P.; Penniger, J. M. L.; Eds. *Supercritical Fluid Science and Technology*; ACS Symposium Series 406; American Chemical Society: Washington, DC, 1989.
(2) Bruno, T. J.; Ely, J. F. *Supercritical Fluid Technology-Reviews in Modern Theory and Applications*; CRC Press: Boca Raton, FL, 1991.
(3) Bright, F. V.; McNally, M. E. P.; Eds. *Supercritical Fluid Technology-Theoretical And Applied Approaches in Analytical Chemistry*; ACS Symposium Series 488; American Chemical Society; Washington, DC, 1992.
(4) Kiran, E.; Brennecke, J. F.; Eds. *Supercritical Fluid Engineering Science-Fundamentals and Applications*; ACS Symposium Series 514; American Chemical Society: Washington, DC, 1993.
(5) McHugh, M. A.; Krukonis, V. J. *Supercritical Fluid Extraction: Principles and Practice*, 2nd ed.; Butterworth-Heinemann: Boston, 1994.
(6) Kiran, E. In *Supercritical Fluids. Fundamentals for Applications*; Kiran, E., Sengers, J. M. H. L., Eds.; Kluwer Academic: Dordrecht, The Netherlands, 1994.
(7) Taylor, L. T. *Supercritical Fluid Extraction*; John Wiley & Sons: New York, 1996.
(8) Jessop, P. G.; Leitner, W. *Chemical Synthesis Using Supercritical Fluids*; Wiley-VCH: Weinheim, Germany, 1999.
(9) Eckert, C. A.; Knutson, B. L.; Debenedetti, P. G. *Nature* **1996**, *383*, 313.
(10) Laintz, K. E.; Wai, C. M.; Yonker, C. R.; Smith, R. D. *J. Supercrit. Fluids* **1991**, *4*, 194.
(11) DeSimone, J. M.; Guan, Z.; Elsbernd, C. S. *Science* **1992**, *257*, 945.
(12) DeSimone, J. M.; Maury, E.; Menceloglu, Y. Z.; Combes, J. R.; McLain, J. B.; Romack, T. J. *Science* **1994**, *265*, 356.
(13) DeSimone, J. M.; Guan, Z.; Combes, J. R.; Menceloglu, Y. Z. *Macromolecules* **1993**, *26*, 2663.
(14) Adamsky, F.; Beckman, E. *Macromolecules* **1994**, *27*, 312.
(15) Consani, K.; Smith, R. *J. Supercrit. Fluids* **1990**, *3*, 51.
(16) Hoefling, T.; Stofesky, D.; Reid, M.; Beckman, E.; Enick, R. *J. Supercrit. Fluids* **1992**, *5*, 237.
(17) Hoefling, T.; Newman, D.; Enick, R.; Beckman, E. *J. Supercrit. Fluids* **1993**, *6*, 165.
(18) Hoefling, T.; Newman, D.; Enick, R.; Beckman, E. *J. Supercrit. Fluids* **1993**, *6*, 205.
(19) Sarbu, T.; Styranec, T.; Beckman E. J. *Nature* **2000**, *405*, 165.
(20) Sarbu, T.; Styranec, T.; Beckman, E. J. *Ind. Eng. Chem. Res.* **2000**, *39*, 4678.
(21) Yazdi, A. V.; Beckman, E. J. *J. Mater. Res.* **1995**, *10*, 530.
(22) Powell, C. J.; Beckman, E. J. *Ind. Eng. Chem. Res.* **2001**, *40*, 2897.
(23) Panza, J. L.; Russel, A. J.; Beckman, E. J. *Tetrahedron* **2002**, *58*, 4091.
(24) Huang, Z.; Shi, C.; Xu, J.; Kilic, S.; Enick, R. M.; Beckman, E. J. *Macromolecules* **2000**, *33*, 5437.
(25) Shi, C.; Huang, Z.; Beckman, E. J.; Enick, R. M.; Kim S.; Curran, D. P. *Ind. Eng. Chem. Res.* **2001**, *40*, 908.
(26) Harrison, K. L.; da Rocha, S. R. P.; Yates, M. Z.; Johnston, K. P.; Canelas D.; DeSimone, J. M. *Langmuir* **1998**, *14*, 6855.
(27) Johnston, K. P. *Curr. Opin. Colloid Interface Sci.* **2000**, *5*, 351.
(28) Liu, J.; Han, B.; Wang, Z.; Zhang, J.; Li. G.; Yang, G. *Langmuir* **2002**, *18*, 3086.
(29) daRocha, S. R. P.; Dickson, J.; Cho, D.; Rossky, P. J.; Johnston, K. P. *Langmuir* **2003**, *19*, 3114.
(30) Sagisaka, M.; Yoda, S.; Takebayashi, Y.; Otake, K.; Kitiyanan, B.; Kondo, Y.; Yoshino, N.; Takebayashi, K.; Sakai, H.; Abe, M. *Langmuir* **2003**, *19*, 220.
(31) Johnston, K. P.; Harrison, K. L.; Clarke, M. J.; Howdle, S. M.; Heitz, M. P.; Bright, F. V.; Carlier, C.; Randolph, T. W. *Science* **1996**, *271*, 624.
(32) Valeur, B.; Monnerie, L. *J. Polym. Sci., Polym. Phys. Ed.* **1976**, *14*, 11.
(33) Phillips, D. *Polymer Photophysics: Luminescence, Energy Migration, and Molecular Motion in Synthetic Polymers*; Chapman and Hall: New York, 1985.
(34) Winnik, M. A. In *Photophysical and Photochemical Tools in Polymer Science*; Winnik, M. A., Ed.; Reidel: Dordrecht, The Netherlands, 1986; pp 467−494.
(35) Hoyle, C. E.; Torkelson, J. M.; Eds. *Photophysics of Polymers*; ACS Symposium Series; American Chemical Society: Washington, DC, 1987; Vol. 358.
(36) Char, K.; Gast, A. P.; Frank, C. W. *Langmuir* **1988**, *4*, 989.
(37) Sasaki, T.; Yamamoto, M. *Macromolecules* **1989**, *22*, 4009.
(38) Ediger, M. D. *Annu. Rev. Phys. Chem*. **1991**, *42*, 225.
(39) Waldow, D. A.; Ediger, M. D.; Yamaguchi, Y.; Matsushita, Y.; Noda, I. *Macromolecules* **1991**, *24*, 3147.
(40) Németh, S.; Jao, T.-C.; Fendler, J. H. *Macromolecules* **1994**, *27*, 5449.
(41) Asano, M.; Winnik, F. M.; Yamashita, T.; Horie, K. *Macromolecules* **1995**, *28*, 5861.
(42) Niemeyer, E. D.; Bright, F. V. *Macromolecules* **1998**, *31*, 71.
(43) Kane, M. A.; Baker, G. A.; Pandey, S.; Maziarz, E. P., III; Hoth, D. C.; Bright, F. V. *J. Phys. Chem. B* **2000**, *104*, 8585.
(44) Stein, A. D.; Hoffman, D. A.; Frank, C. W.; Fayer, M. D. *J. Chem. Phys*. **1992**, *96*, 3269.
(45) Leezenberg, P. B.; Marcus, A. H.; Frank, C. W.; Fayer, M. D. *J. Phys. Chem*. **1996**, *100*, 7646.
(46) Munson, C. A.; Kane, M. A.; Baker, G. A.; Pandey, S.; Perez, S. A.; Bright, F. V. *Macromolecules* **2001**, *34*, 4624.
(47) Shaffer, K. A.; Jones, T. A.; Canelas, D. A.; DeSimone, J. M.; Wilkinson, S. P. *Macromolecules* **1996**, *29*, 2704.
(48) Yates, M. Z.; Shah, P. S.; Johnston, K. P.; Lim, K. T.; Webber, S. *J. Colloid Interface Sci.* **2000**, *227*, 176.
(49) Kane, M. A.; Pandey, S.; Baker, G. A.; Perez, S. A.; Bukowski, E. J.; Hoth, D. C.; Bright, F. V. *Macromolecules* **2001**, *34*, 6831.
(50) Gardinier, W. E.; Kane, M. A.; Bright, F. V. *J. Phys. Chem. B* **2004**, *108*, 18520.
(51) Elias, H. G. In *Polymer Handbook*, 3rd ed.; Brandrup, J., Immergut, E. H., Eds.; John Wiley and Sons: New York, 1989; Vol. II.
(52) (a) Lakowicz, J. R. *Principles of Fluorescence Spectroscopy*, 2nd ed.; Kluwer Academic/Plenum Publishers: New York, 1999. (b) Steiner, R. F. In *Topics in Fluorescence Spectroscopy*; Lakowicz, J. R., Ed.; Plenum Press: New York, 1991; Vol. 3, pp 1−52. (c) Perrin, F. *J. Phys. Radium V, Ser. 6* **1926**, *7*, 390. (d) Perrin, F. *Ann. Phys., Ser. 10* **1929**, *12*, 169.
(53) (a) Berghmans, M.; Govaers, S.; Berghmans, H.; De Schryver, F. C. *Polym. Eng. Sci.* **1992**, *32*, 1466. (b) Morita, S.; Tsunomori, F.; Ushiki, H. *Eur. Polym. J.* **2002**, *38*, 1863. (c) Nichifor, M.; Lopes, S.; Bastos, M.; Lopes, A. *J. Phys. Chem. B* **2004**, *108*, 16463.

(54) In cases where a relatively small fluorescent probe is attached to a larger macromolecule, the observed steady-state fluorescence anisotropy from the probe results from a combination of local probe motion, segmental motion of a subregion of the entire macromolecule and the probe, and/or the global motion of the macromolecule.[52a,b] As a result, if there is local/segmental dynamics, which is likely here, the measured experimental steady-state fluorescence anisotropy is biased toward lower values in comparison to what the value would be if the probe did not undergo local/segmental motion. Thus, the steady-state anisotropy measurements tend to underestimate intermolecular association if the associating species are flexible and the probe can undergo motion independent of the macromolecule.[52a,b,53]
(55) Hu, Y.; Horie, K.; Ushiki, H. *Macromolecules* **1992**, *25*, 6040.
(56) Spencer, R. D.; Weber, G. *J. Chem. Phys.* **1970**, *52*, 1654.
(57) Betts, T. A.; Bright, F. V. *Appl. Spectrosc.* **1990**, *44*, 1196.
(58) Equation of State for Windows 95, programmed by David Bush, Georgia Institute of Technology, 1997.
(59) Fenghour, A.; Wakeham, W. A.; Vesovic, V. *J. Phys. Chem. Ref. Data* **1998**, *27*, 31.
(60) Tilly, K. D.; Foster, N. R.; Macnaughton, S. J.; Tomasko, D. L. *Ind. Eng. Chem. Res.* **1994**, *33*, 681.
(61) (a) Li, Y. H.; Chan, L.-M.; Tyer, L.; Moody, R. T.; Himel, C. M.; Hercules, D. M. *J. Am. Chem. Soc.* **1975**, *97*, 3118. (b) Lochmüller, C. H.; Marshall, D. B.; Wilder, D. R. *Anal. Chim. Acta* **1981**, *130*, 31. (c) Lochmüller, C. H.; Marshall, D. E.; Harris, J. M. *Anal. Chim. Acta* **1981**, *131*, 263. (d) Kosower, E. M. *Acc. Chem. Res.* **1982**, *15*, 259. (e) Rettig, W. *Angew Chem., Int. Ed. Engl.* **1986**, *25*, 971. (f) Holmes-Farley, S. R.; Whitesides, G. M. *Langmuir* **1986**, *2*, 266. (g) Shea, K. J.; Sasaki, D. Y.; Stoddard, G. J. *Macromolecules* **1989**, *22*, 1722. (h) Men, Y.; Marshall, D. B. *Anal. Chem.* **1990**, *62*, 2606. (i) Reichardt, C. *Chem. Soc. Rev.* **1992**, 147. (j) Leezenberg, P. B.; Frank, C. W. *Chem. Mater.* **1995**, *7*, 1784. (k) Gonzalez-Benito, J.; Cabanelas, J. C.; Aznar, A. J.; Vigil, M. R.; Bravo, J.; Baselga, J. *J. Appl. Polym. Sci.* **1996**, *62*, 375. (l) Pandey, S.; Baker, G. A.; Kane, M. A.; Bonzagni, N. J.; Bright, F. V. *Chem. Mater.* **2000**, *12*, 3547. (m) Gonzalez-Benito, J.; Aznar, A.; Baselga, J. *J. Fluoresc.* **2001**, *11*, 307.
(62) Melnichenko, Y. B.; Kiran, E.; Wignall, G. D., Heath, K. D.; Salaniwal, S.; Cochran, H. D.; Stamm, M. *Macromolecules* **1999**, *32*, 5344.
(63) (a) James, D. J.; Ware, W. R. *Chem. Phys. Lett.* **1985**, *120*, 455. (b) James, D. J.; Liu, Y. S.; DeMayo, P.; Ware, W. R. *Chem. Phys. Lett.* **1985**, *120*, 455. (c) James, D. J.; Ware, W. R. *Chem. Phys. Lett.* **1986**, *126*, 7. (d) Alcala, J. R.; Gratton, E.; Predergast, F. G. *Biophys. J.* **1987**, *51*, 587. (e) Alcala, J. R.; Gratton, E.; Predergast, F. G. *Biophys. J.* **1987**, *51*, 597. (f) Gryczynski, I.; Wiczk, W.; Johnson, M. L.; Lakowicz, J. R. *Biophys. Chem.* **1988**, *32*, 173. (g) Huang, J.; Bright, F. V. *J. Phys. Chem.* **1990**, *94*, 8457. (h) Bright, F. V.; Catena, G. C.; Huang, J. *J. Am. Chem. Soc.* **1990**, *112*, 1343.
(64) *Silicon Compounds. Register and Review*; United Chemical Technologies, pp 254−255.
(65) Pandey, S.; Kane, M. A.; Baker, G. A.; Bright, F. V.; Fürstner, A.; Seidel, G.; Leitner, W *J. Phys. Chem. B* **2002** *106*, 1820.

MA047989K